

Showcasing research from the Max Planck Institute for Chemical Energy Conversion and the group of Professor Jennifer Strunk, Leibniz Institute for Catalysis, Germany

The fate of O₂ in photocatalytic CO₂ reduction on TiO₂ under conditions of highest purity

This study is dedicated to understanding the often-reported absence of gaseous O₂ during photocatalytic conversion of CO₂ and H₂O to CH₄ over TiO₂-photocatalysts. While IrO_x-modified P25-TiO₂ allowed the detection of O₂ and H₂ in almost stoichiometric amounts, the results simultaneously imply that hydrogen for the CH₄ formation does not result from complete water oxidation. A lack of gaseous O₂ over unmodified P25-TiO₂ stems from a consumption of O-derived species by TiO₂.

As featured in:



See Simon Ristig,
Jennifer Strunk et al.,
Phys. Chem. Chem. Phys.,
2019, **21**, 15949.



ROYAL SOCIETY
OF CHEMISTRY | Celebrating
IYPT 2019

rsc.li/pccp

Registered charity number: 207890



Cite this: *Phys. Chem. Chem. Phys.*,
2019, 21, 15949

The fate of O₂ in photocatalytic CO₂ reduction on TiO₂ under conditions of highest purity†

Martin Dilla,^a Alina Jakubowski,^a Simon Ristig, ^{a*} Jennifer Strunk ^{b*} and Robert Schlögl^{ac}

Although the photocatalytic reduction of CO₂ to CH₄ by using H₂O as the oxidant presupposes the formation of O₂, it is often not included in the product analysis of most of the studies dealing with photocatalytic CO₂ reduction or it is reported to be not formed at all. The present study aims to clarify the absence of O₂ in the photocatalytic gas phase CO₂ reduction on TiO₂. By modifying P25-TiO₂ with IrO_x co-catalysts it was possible to observe photocatalytic water splitting, *i.e.* the formation of gaseous O₂ and H₂ in almost stoichiometric amounts, without the use of sacrificial agents, while bare P25-TiO₂ showed no activity in H₂ and O₂ formation under similar reaction conditions. Investigating the effect of improved H₂O oxidation properties on the photocatalytic CO₂ reduction revealed that the CH₄ formation on P25 from CO₂ was completely inhibited as long as the H₂O splitting reaction proceeded. Furthermore, we found that a certain amount of O₂ is consumed under conditions of photocatalytic water oxidation. A quantification showed it to be in the same order of magnitude as the oxygen which is missing as a byproduct from photocatalytic CO₂ conversion. A detailed interpretation of the results in the context of the general understanding of the photocatalytic CO₂ reduction with H₂O on TiO₂ allows the hypothesis that P25-TiO₂ undergoes a stoichiometric reaction, meaning that the CH₄ formation is not based on a true catalytic cycle and runs only as long as TiO₂ can consume oxygen.

Received 20th December 2018,
Accepted 1st May 2019

DOI: 10.1039/c8cp07765g

rsc.li/pccp

Introduction

The photocatalytic reduction of CO₂ attracted lots of attention within the last thirty years. Forming mobile energy sources by chemical reactions with CO₂ and the help of (sun-)light would be an important achievement for a more sustainable energy system that helps to protect the environment.¹ Due to the massive use of fossil fuels for energy supply and the depletion of natural reservoirs in the near future,² it is desirable to commercialize alternative ways for providing humanity with renewable energy sources.³ Another important issue is the noticeable accumulation of CO₂ in the atmosphere as a result of the total combustion of fossil fuels.^{3,4} An increasing CO₂ level accelerates the greenhouse effect and is associated with global warming and changes of the climatic conditions. Making use of CO₂ as a raw material could contribute to decreasing the production of anthropogenic CO₂ and help to use carbon-containing

energy carriers in a closed cycle. An often used term for such a reaction is “artificial photosynthesis”.⁵

An efficient photocatalyst needs to perform at least two functions. The first function is that of a photoabsorber, which means that the material generates charge carriers upon absorption of photons. These charge carriers must have adequate oxidation and reduction potential for the desired redox reactions.^{6,7} It is also necessary that the charge carriers become spatially separated from each other to avoid their immediate recombination, and that they can migrate to the surface of the material. The second function is that of a heterogeneous catalyst. Therefore, it is necessary that the material exposes active sites in order to activate the reactants sufficiently to facilitate charge carrier transfer reactions. Such an activation can be initiated by adsorption of the reactants on the catalyst surface.⁸ After decades of research TiO₂ is still one of the most promising and most studied materials as photocatalyst for reduction of CO₂.¹ Indeed a number of alternative materials have been tried, but the activity of TiO₂,⁹ the non-toxicity, stability against photocorrosion^{10,11} and the commercial availability maintain it as a meaningful candidate for photocatalytic approaches. However, performing photocatalytic CO₂ reduction experiments in order to gain knowledge about the mechanistic details is a challenge.^{12,13} The examination of elementary steps, for instance, the identification of kinetic barriers or the finding

^a Max Planck Institute for Chemical Energy Conversion,
45470 Mülheim an der Ruhr, Germany. E-mail: simon.ristig@cec.mpg.de

^b Leibniz Institute for Catalysis, 18059 Rostock, Germany.
E-mail: jennifer.strunk@catalysis.de

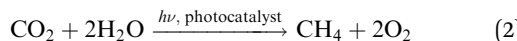
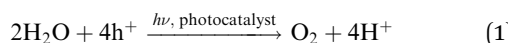
^c Fritz Haber Institute of the Max Planck Society, 14195 Berlin, Germany

† Electronic supplementary information (ESI) available. See DOI: 10.1039/c8cp07765g



of details about the structure–function relationships of photocatalysts is often limited by their low activity in product formation and the detection limit of many standard analytical methods and tools.¹⁴ For this reason the mechanism of this highly complex reaction is not well understood.^{15–18}

In many reports the main products of photocatalytic CO₂ reduction are CH₄, CO and methanol.^{14,19–21} Given that CH₄ is formed from CO₂ in a photocatalytic reduction, it is necessary that the C=O double bonds are cleaved and four C–H bonds are formed. This process requires the transfer of eight electrons from TiO₂ to the carbon atom. For this reason a second reactant, which can provide these charge carriers and the source of hydrogen is needed. H₂O is the most desirable oxidant for this purpose. It is commonly believed that the process of photocatalytic H₂O oxidation on TiO₂ is associated with the transfer of four holes (h⁺) to form an O₂ molecule (1). At the same time the bound hydrogen is liberated for a subsequent hydrogenation reaction (1).



Both processes, the reduction of CO₂ and the oxidation of H₂O produce excess oxygen as by-product which is expected to desorb from the catalyst as molecular O₂. It is proposed that this excess oxygen is converted to O₂ (2). In the end the overall photocatalytic CO₂ reduction with H₂O results in the formation of two equivalents of O₂ per CH₄ molecule (2). However, with some exceptions^{22–26} the research effort focuses mostly on the formation of carbon-related products, probably as they are the targeted product for storing chemical energy. The formation of O₂ is often neglected, or it cannot be found at all in the products of photocatalytic CO₂ reduction.^{27,28} The absence of O₂ can have several reasons, for instance, the participation in the backwards reaction (CH₄ oxidation), the replenishment of oxygen vacancies (O_V) on TiO₂^{29,30} and limitations in H₂O oxidation kinetics leading to the accumulation of reaction intermediates on the catalyst surface. The latter could be related to the overpotential of H₂O oxidation on bare TiO₂.³¹ Without using an external bias the activity towards H₂O oxidation might be rather low. Then it would be questionable if there is any other hydrogen source for C–H bond formation, such as surface hydroxyl groups.

In our previous studies^{32,33} we performed continuous flow CO₂ reduction experiments where we demonstrated that CH₄ formation is dependent on the availability of CO₂ and H₂O. Without dosing of H₂O, the product formation diminished after a couple of hours and initiated again as a pulse of H₂O was given into the reactor. It was concluded that the reaction proceeds initially by the contribution of physisorbed H₂O residues, which are usually available on the surface of TiO₂.^{34,35} The product formation ceases once they are consumed for hydrogenation or light-induced thermal desorption. Then the pulse-dosed H₂O molecules serve as the source of hydrogenation. Although H₂O appears to participate in the photoinduced CH₄

formation, it was not possible to detect any O₂ or oxygen-derived species as products of H₂O oxidation. On this account the present study focuses on the clarification of the fate of O₂ as the by-product of the overall photocatalytic CO₂ reduction.

The most prominent materials for H₂O oxidation in electrochemical approaches are IrO_x and CoO_x. It has been found that these transition metal oxides exhibit an outstanding activity in this reaction because of their relatively low overpotential.^{36–39} Investigations on IrO_x and CoO_x materials have shown that the activity in the OER is dependent on the concentration of lattice defects.^{36,40} A study on hydrated amorphous Ir oxyhydrates⁴⁰ revealed that IrO_x species having defects in the cationic and anionic lattice structure are more active in the OER. The authors concluded that weakly bound electrophilic oxygen species play a key role in the superior activity. In order to form such electrophilic oxygen species the surrounding Ir lattice requires flexible oxidation states.⁴⁰ The electrophilic oxygen species are prone to nucleophilic attacks of H₂O. It is assumed that these species participate in the potential limiting step, namely the O–O bond formation of the OER.^{40,41} Furthermore the photocatalytic activity of IrO_x as a co-catalyst for the O₂ evolution reaction has also been tested. It is proposed that photogenerated holes in TiO₂ are transferred to the IrO_x particles,^{42,43} where the H₂O oxidation reaction takes place. In this way TiO₂ represents the photoabsorber and IrO_x the heterogeneous catalyst. Such IrO_x/TiO₂ materials showed an improved O₂ evolution activity compared to bare TiO₂.⁴² On this account it appears to be a suitable candidate for modification of P25 TiO₂ with an O₂ evolution co-catalyst, in order to evaluate if improved H₂O oxidation conditions have an effect towards the overall product formation of photocatalytic CO₂ reduction to CH₄. At the same time the impact of O₂ evolution on CH₄ formation can be investigated. This elucidation helps to verify if product formation is a true catalytic cycle. Furthermore, it contributes to a better understanding of this complicated process and assists the development of reaction-based modification strategies for photocatalyst preparation.

Results

Photocatalytic cleaning and H₂O splitting with IrO_x/P25

The results of photocatalytic H₂O splitting experiments with the 0.05 wt% IrO_x/P25 samples calcined at 400 and 200 °C, respectively are shown in Fig. 1 and 2. A significant H₂ formation can be observed for both samples once the illumination is started at 0 h (Fig. 1 and 2). It can also be seen that the H₂ formation rates scale with the flow rates of H₂O and stabilize over the course of the experiment. In contrast O₂ formation shows a different development. O₂ is only detected after 6 h of illumination in the first experiment of the 400 °C sample (Fig. 1A). For this reason a second H₂O splitting experiment with this sample is conducted (Fig. 1B). In this experiment the apparent O₂ formation rate increases strongly from 0 to 3.75 h. From 3.75 h on, the formation rate of O₂ appears to be unsteady and the ratio between the evolution of O₂ and H₂ is approximately 1:3.



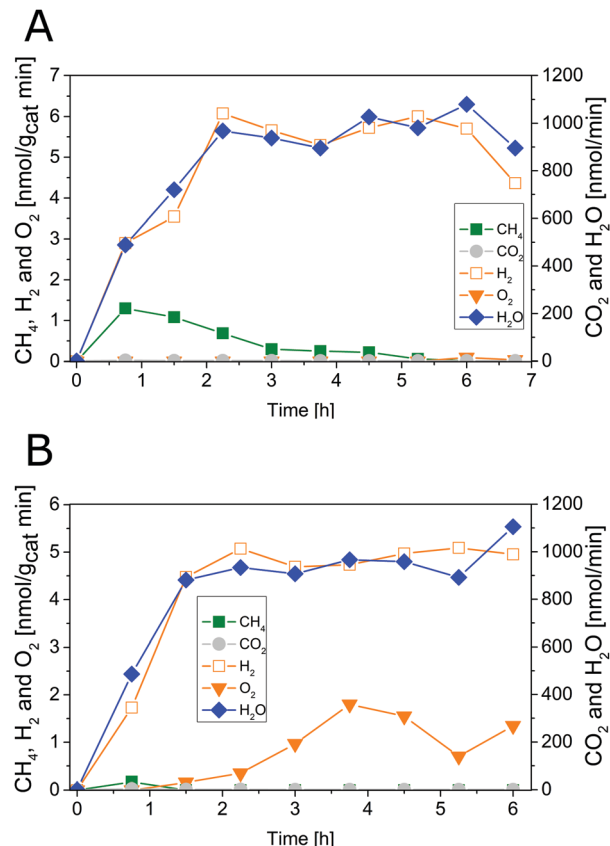


Fig. 1 Photocatalytic H_2O splitting with 0.05 wt% $\text{IrO}_x/\text{P25}$ calcined at 400 °C, irradiation time: 6.75 h; (A) first experiment, (B) second experiment. Lines are included in order to guide the eye.

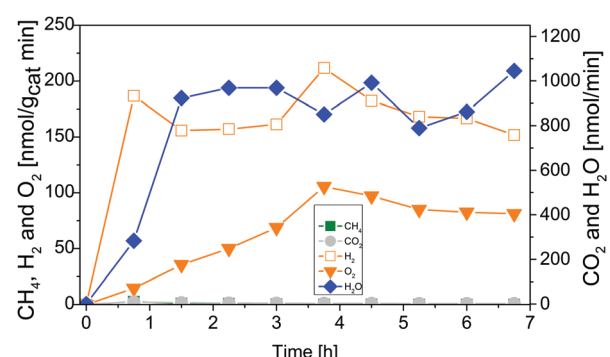


Fig. 2 Photocatalytic H_2O splitting with 0.05 wt% $\text{IrO}_x/\text{P25}$ calcined at 200 °C. Irradiation time: 6.75 h. Lines are included in order to guide the eye.

The 200 °C calcined sample shows also an increase of the apparent O_2 formation rate from 0 to 3.75 h (Fig. 2). Moreover, the product formation rates after 3.75 h reveal a $\text{O}_2:\text{H}_2$ ratio of approximately 1:2.

From 5.25 to 6.75 h (Fig. 2) the product formation becomes relatively stable so that steady-state conditions are almost reached. However, it is questionable why the apparent O_2 formation starts delayed to the H_2 formation. Another important observation is the difference in the overall activity

of the two samples. It can be noticed that the 200 °C sample is about 30 times more active in H_2 formation than the 400 °C sample. Thus, the calcination temperature seems to have a distinct influence on the catalytic properties of the $\text{IrO}_x/\text{P25}$ samples.

The reference P25 samples were also tested with respect to their performance in photocatalytic H_2O splitting. From Fig. 3A and B it can be observed that the samples show no measurable activity in the formation of O_2 and H_2 . The results of the modified samples indicate that IrO_x positively influences the formation of H_2 and O_2 .

Photocatalytic cleaning and H_2O splitting with $\text{CoO}_x/\text{P25}$

In contrast to the IrO_x -modified P25 samples, the CoO_x modified samples show a significantly different activity in the photocatalytic H_2O splitting reaction. From Fig. S1A and B (ESI†) it can be observed that only the sample calcined at 200 °C showed activity in H_2 formation. Furthermore it can be seen that the activity in H_2 formation ceases over the time of illumination (Fig. S1A, ESI†). Both samples, the 200 °C and 400 °C sample, did not exhibit any activity in O_2 formation. The 400 °C samples displayed no activity in the H_2 and O_2 formation. Due to the absence of activity in O_2 formation, the samples were not further tested in the photocatalytic CO_2 reduction.

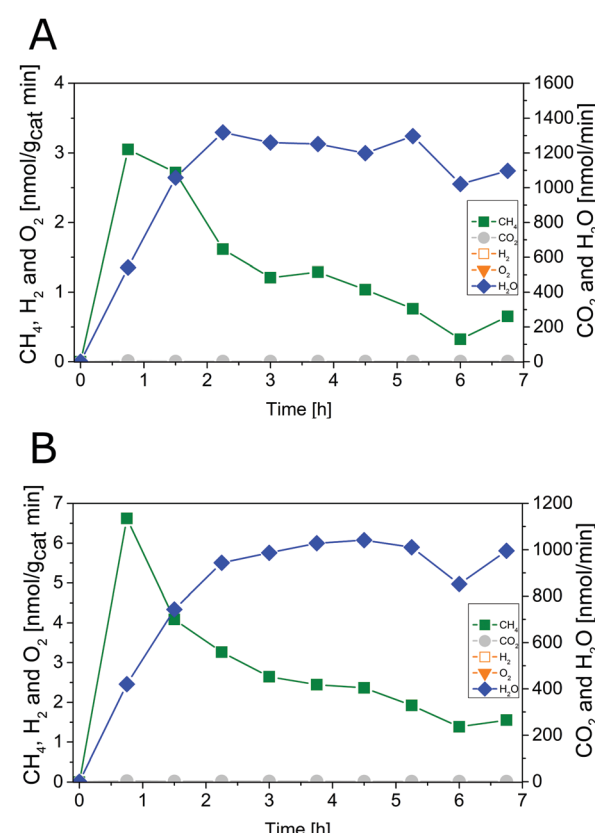


Fig. 3 Photocatalytic H_2O splitting with (A) P25 reference sample calcined at 200 °C. (B) P25 reference sample calcined at 400 °C. Irradiation time: 6.75 h. Lines are included in order to guide the eye.

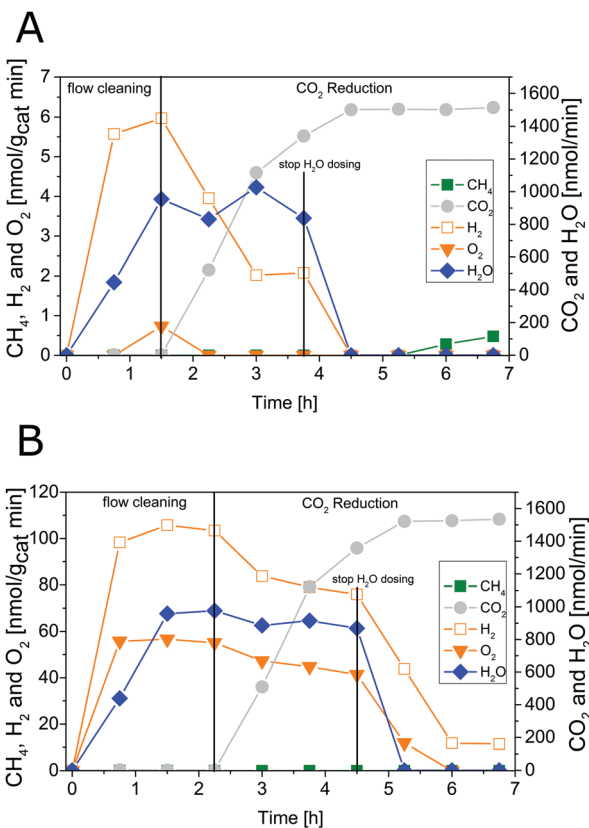


Fig. 4 Photocatalytic CO_2 reduction with 0.05 wt% $\text{IrO}_x/\text{P25}$ calcined at (A) 400 °C (flow cleaning from 0 to 1.5 h, CO_2 reduction from 1.5 h to 6.75 h, H_2O dosing from 0 to 3.75 h) and (B) 200 °C (flow cleaning from 0 to 2.25 h, CO_2 reduction from 2.25 h to 6.75 h, H_2O dosing from 0 to 4.5 h). Lines are included in order to guide the eye.

Photocatalytic CO_2 reduction with $\text{IrO}_x/\text{P25}$

Fig. 4 shows results of combined flow cleaning and photocatalytic CO_2 reduction experiments with the $\text{IrO}_x/\text{P25}$ samples. Both samples show significant activity in the formation of H_2 and O_2 before the CO_2 dosing was initiated. The formation rate of these products decreases once CO_2 is flushed through the reactor, although the water concentration remained fairly constant. In case of the sample calcined at 400 °C the rate of H_2 was more than halved within 3.25 h of CO_2 dosing, while O_2 was completely absent (Fig. 4A) in the products. These observations are less pronounced for the 200 °C sample (Fig. 4B) so that only a slight decrease of both rates was observed. However, under the applied reaction conditions it was not possible to detect CH_4 as a product of CO_2 reduction. It rather seems that CO_2 has primarily a negative impact on the H_2 and O_2 formation in a way that generation of products is markedly disturbed. The dosing of H_2O was stopped after 3.25 h of CO_2 reduction, to probe if the absence of this reactant makes a difference in the overall selectivity. From Fig. 4 it can be seen that the absence of H_2O in the gas flow strongly affects the H_2 and O_2 formation. A clear decrease of both formation rates can be seen. More specific, it can be noticed that no H_2 and O_2 evolution takes place for the 400 °C sample. In case of the 200 °C sample, the O_2 formation declines completely while that of H_2 drops down to a

constant rate. However, after the H_2O dosing was stopped it was possible to observe formation of CH_4 , at least for the 400 °C sample. Thereby the rate increased from 5.25 to 6.75 h (Fig. 4A). In contrast the 200 °C sample showed no CH_4 formation under the applied reaction conditions.

The intensive dosing of H_2O during activity studies could result in an accumulation of this reactant on the surface of TiO_2 based photocatalysts, which can limit its activity in CO_2 reduction.³² In order to investigate this potential limitation, a similar experiment with the 200 °C sample was carried out with a reduced H_2O flow rate of $\sim 25 \text{ nmol min}^{-1}$. With these conditions bare P25 showed the highest CO_2 reduction activity in our previous studies.³² The results of the flow cleaning and CO_2 reduction experiments are displayed in Fig. S2 (ESI†) and Fig. 5, respectively, and reveal a significant activity in the H_2 and O_2 formation with the reduced amounts of H_2O . After adding CO_2 to the gas flow the apparent O_2 formation ceases completely, while H_2 formation decreases to a stable rate. It was again not possible to detect any CH_4 formation (Fig. 5). The pure P25 references, without IrO_x or CoO_x , showed significant activity in CH_4 formation when CO_2 was given to the reactor (Fig. S3A and B, ESI†). The activity of the sample calcined at 200 °C (Fig. S3A, ESI†) was higher than that of the 400 °C sample (Fig. S3B, ESI†). This observation is similar to the activity of the $\text{IrO}_x/\text{P25}$ samples in H_2O splitting (Fig. 1 and 2). The P25 reference samples however exhibited no activity in H_2 and O_2 formation at all (Fig. 3). These findings are in accordance with our previous studies on photocatalytic CO_2 reduction with P25.^{32,33} In a consecutive experiment with the P25 references it was investigated if a similarly delayed initiation of O_2 evolution can be observed during CH_4 formation, as it was observed for the $\text{IrO}_x/\text{P25}$ samples. Therefore a combined flow cleaning and CO_2 reduction experiment was carried out with the sample calcined at 400 °C (Fig. 6) for an extended period of 18 h. To prevent an inhibition of CH_4 formation by extensive accumulation or a complete lack of H_2O , repetitive pulse dosing of H_2O was performed in order to provide suitable conditions to run CH_4 formation over an appropriate period of time. It can be obviously seen in Fig. 6 that after about 6 h the pulses of H_2O initially decrease the rate of CH_4 formation.

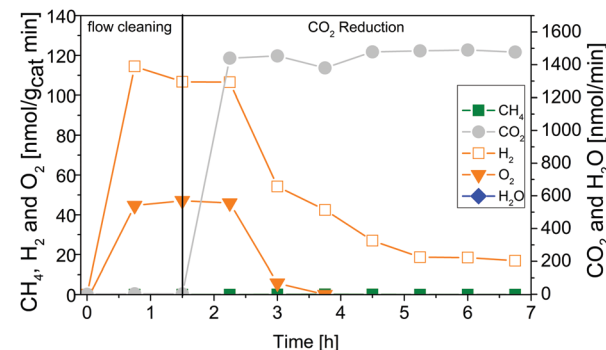


Fig. 5 Photocatalytic CO_2 reduction with 0.05 wt% $\text{IrO}_x/\text{P25}$ calcined at 200 °C (flow cleaning from 0 to 1.5 h, CO_2 reduction from 1.5 h to 6.75 h, $\sim 25 \text{ nmol min}^{-1}$ H_2O dosing from 0 to 6.75 h). Lines are included in order to guide the eye.



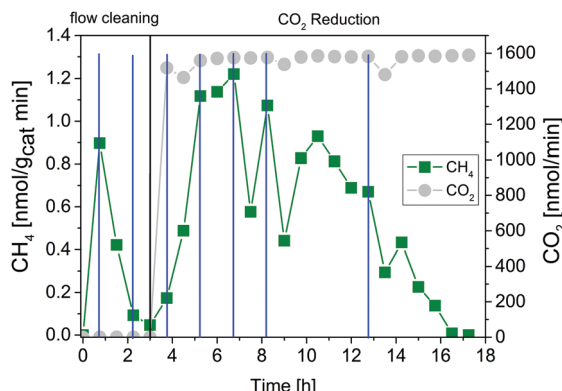


Fig. 6 Photocatalytic CO_2 reduction with P25 calcined at 400 °C (flow cleaning from 0 to 3 h, CO_2 reduction from 3 h to 17.75 h, pulse dosing of H_2O indicated by blue dashes). Lines are included in order to guide the eye.

However, a significant increase of the CH_4 formation can be observed in each of the subsequent GC analysis cycles. In total it was possible to observe CH_4 formation over a period of 14.25 h (Fig. 6). Under the applied reaction conditions the CH_4 formation rate decreases over the course of the CO_2 reduction experiment. There was no activity left after 17.75 h (Fig. 6). As no delayed O_2 formation could be detected during the experiment it seems that, in contrast to the H_2O splitting experiments on $\text{IrO}_x/\text{P25}$, bare P25 does not release any molecular oxygen in a similar range of time.

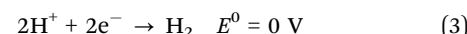
Discussion

The results can be discussed in the context of the general understanding of photocatalytic energy conversion reactions on TiO_2 -based materials. Then, a detailed insight into the mode of action can be obtained for $\text{IrO}_x/\text{TiO}_2$ and some hypotheses on the reaction progress on TiO_2 can be formulated.

Photocatalytic cleaning and H_2O splitting on $\text{IrO}_x/\text{P25}$

The IrO_x -modified P25 samples showed a noticeable activity in the formation of H_2 and O_2 . Due to the strong dependence of the activity from the dosing of H_2O and the $\text{O}_2:\text{H}_2$ ratio of approximately 1:2, it is assumed that the product formation originates from overall photocatalytic H_2O splitting (4). This is a meaningful result showing that the stoichiometric H_2O splitting in a gas-solid process has been realized, since no external bias or any sacrificial agents were used in order to improve the formation rates of H_2 and O_2 . Furthermore, it is possible to observe the simultaneous formation of both products in one high-purity reaction chamber. However, it is questionable how the product formation is realized on $\text{IrO}_x/\text{P25}$ and which charge carrier dynamic processes are involved. A hypothetical approach to explain the activity of $\text{IrO}_x/\text{P25}$ can be based on the two main functions of a photocatalyst. In this sense TiO_2 represents the photoabsorber, where mobile charge carriers are generated under absorption of UV photons. Some of the photogenerated h^+ escape from recombination and migrate to the IrO_x particles, where they catalyze the oxidation of H_2O to O_2 (1). In this way IrO_x represents the function of the

heterogeneous catalyst. This has been well documented in liquid-phase H_2O splitting. The separation of charge carriers over the interface of TiO_2 and IrO_x enhances their lifetime, thus it is beneficial for the light efficiency of the overall H_2O splitting reaction (4). The H^+ formed from H_2O oxidation (1) are then reduced to H_2 gas (3). Since the electrons are left behind in TiO_2 , this reaction is likely to proceed on the TiO_2 surface. For this purpose TiO_2 must expose sites which can transfer electrons. It appears that such sites are available and their accessibility is maintained even under continuous flow conditions and accumulation of H_2O on the surface of TiO_2 , since the activity of H_2 formation is almost stable during the H_2O splitting experiments.



With respect to H_2 formation, the catalytic functionality is inherent to TiO_2 , as has been observed earlier, and a modification with a co-catalyst does not seem to be needed to generally allow this reaction.⁴⁴ The functionalization of TiO_2 with co-catalysts, especially Pt, is however a common approach to improve the H_2 formation capability for significantly higher H_2 yields.⁴⁵

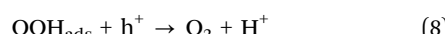
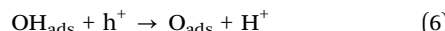
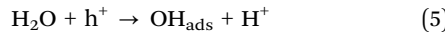
According to the hypothetical approach in the previous chapter to explain the activity of $\text{IrO}_x/\text{P25}$ it is expected that the H_2O oxidation reaction similarly proceeds on CoO_x and the formation of H_2 on TiO_2 . In Fig. S1A and B (ESI[†]) it was shown that only the sample calcined at 200 °C showed activity in H_2 formation. However, the fact that H_2 was formed indicates that a hydrogen source has been provided by photocatalytic H_2O oxidation. The interface between TiO_2 and CoO_x can potentially cause an insufficient hole transfer between the photoabsorber and the co-catalyst which lowers the activity of H_2O oxidation. Furthermore the reaction pathway of photocatalytic H_2O oxidation on CoO_x will be different compared to IrO_x . Therefore it is possible that specific steps in the overall reaction mechanism cannot be activated sufficiently to allow an efficient O_2 formation. As a consequence H_2O is only oxidized partly, so that the resulting oxygen-derived intermediates remain on CoO_x , without being further oxidized to O_2 gas. In this way the oxygen-derived intermediates might prevent further oxidation of H_2O , which lowers the activity over time as it was observed in Fig. S1A (ESI[†]).

Potential reasons for the lack of CH_4 formation on $\text{IrO}_x/\text{TiO}_2$

The CO_2 reduction experiments with the $\text{IrO}_x/\text{P25}$ samples displayed no measurable activity in CH_4 formation. Instead, O_2 and H_2 formation are the dominant processes and only small amounts of CH_4 can be formed if H_2O dosing is stopped (Fig. 4A). This observation is in stark contrast to the reference samples. It is highly probable that the improved H_2O splitting conditions by the IrO_x modification are responsible for the absence of CH_4 formation. In the following it will be elucidated in which ways the H_2O oxidation reaction might affect the CO_2 reduction reaction.

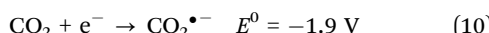
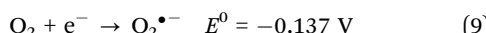


The oxidation of H_2O to O_2 is often represented by four single step reactions (5)–(8).^{31,46–48}



Each of these steps comprises the transfer of one h^+ . Species such as hydroxyl- (5), oxygen adatom- (6) and hydroperoxyl-species (7) are formed as intermediates. Especially the hydroxyl and peroxy species are highly reactive oxygen species and have potential to promote the backward reaction of CO_2 reduction, which is hydrocarbon oxidation.

Aside from hydrocarbon oxidation, another explanation for the absence of CH_4 formation could be based on a competition for charge carriers. For instance the reduction of O_2 (9) and the generation of H_2 (3) are also electron consuming reactions. It is questionable which of these processes is associated with the lowest barrier and is thus more likely to proceed. Due to a lack of knowledge on activation barriers, the redox potentials of the particular reactions are regarded as a first approximation.



For a reaction with CO_2 the commonly proposed one electron transfer⁷ is considered to be the rate limiting step. The comparison of the redox potentials reveals that CO_2 reduction (10) is the thermodynamically least favored process.^{49–51} It needs to be stressed that reaction (10) is virtually not possible thermodynamically on any semiconducting material, because conduction band minima are not located at sufficiently negative potential.⁷ This one electron transfer can only proceed if, for instance, the adsorption of the CO_2 molecule leads to a slightly bent structure, activating the CO_2 and facilitating further reactions. As a consequence of the extreme stability of CO_2 it is highly probable that the photogenerated charge carriers are more likely consumed by H_2 evolution and O_2 reduction, so that fewer electrons are available for reduction of CO_2 . Hence the activity of TiO_2 in CH_4 formation could be negatively influenced. Such a competition for charge carriers would also explain the decrease in water splitting activity of $\text{IrO}_x/\text{TiO}_2$ when CO_2 is added to the reaction mixture (Fig. 4A and 5). In a related manner, bicarbonates, which may be formed in presence of CO_2 on the TiO_2 surface, have been proposed as hole trap sites.⁵² This represents an alternative mechanism by which competition for charge carriers, holes in this case, might occur.

The absence of CH_4 formation in the presence of a highly active co-catalyst for O_2 evolution due to reactive oxygen species and competitive charge transfer reaction appears to be plausible.

As a third possible explanation it should be considered that at least one potential mechanism suggested for CO_2 reduction to CH_4 on TiO_2 , namely the glyoxal pathway,¹⁸ contains not only reductive but also oxidative elementary steps. If such a

mechanism is in operation, it will no longer be possible on TiO_2 if all holes are transferred to IrO_x .

H_2O oxidation on $\text{IrO}_x/\text{TiO}_2$ and fate of oxygen

What makes the results of the $\text{IrO}_x/\text{P25}$ sample significantly more interesting is the activity in the H_2 formation as a consequence of the improved H_2O oxidation properties, together with the delayed O_2 formation rate in the initial phase of the flow cleaning experiments. The obtained results provide specific information about the photocatalytic properties of TiO_2 . Those will later be used to explain product formation of photocatalytic CO_2 reduction on TiO_2 .

The results with $\text{IrO}_x/\text{P25}$ (Fig. 1, 2 and 4) indicated that not all O_2 produced from H_2O oxidation was detected over the course of the experiment. In case of CO_2 reduction on P25 it was even not possible to detect any O_2 . For this reason the deficient amount of O_2 was determined for the $\text{IrO}_x/\text{P25}$ and P25 samples calcined at 400 °C. At first the absent amount of O_2 is calculated for $\text{IrO}_x/\text{P25}$. For this purpose the overall H_2 formation and the $\text{O}_2 : \text{H}_2$ ratio of 1:2 as proposed in reaction (4) are used. The difference between the theoretically expected (O_2 theoretical) and the detected amount (O_2 detected) corresponds to the amount of O_2 which was not found (O_2 absent) in the gas-phase of the photoreactor (Table 1).

In order to realize a reliable comparison to the absent amount of O_2 in CO_2 reduction, it would be necessary to run the reaction until stoichiometric formation of both products can be observed, too. However, the CH_4 formation ceased after 14.25 h of CO_2 reduction (Fig. 6). Consequently it is solely possible to determine the theoretically expected amount of O_2 to this point of time. The calculation was performed under consideration of the stoichiometry in reaction (2). Thereby the molar amount of O_2 corresponds to twice the molar amount of CH_4 (Table 2).

The comparison of the balances (Tables 1 and 2) reveals that the absent amounts of O_2 in both the H_2O splitting reaction with $\text{IrO}_x/\text{P25}$ (Fig. 1) and the CO_2 reduction with bare P25 (Fig. 6) are at least in the same order of magnitude. On this account it appears realistic that the observed phenomena are based on the same effect. The present study uses a GC as the analytical device so that only the gas phase of the photoreactor can be analyzed. Hence, the absence of O_2 in the analysis is either indicative for the absence of its formation or the consumption by the sample.

Table 1 Calculation of absent O_2 in the flow cleaning experiments with the 0.05 wt% $\text{IrO}_x/\text{P25}$ (400 °C); 70 mg of sample was used

	Molar amount [nmol]
H_2	247
O_2 theoretical	123.5
O_2 detected	20
O_2 absent	103.5

Table 2 Calculation of absent O_2 in the flow cleaning experiments with P25 (400 °C); 70 mg of sample was used

	Molar amount [nmol]
CH_4	39
O_2 absent	78



The obtained results are the basis to hypothesize the fate of oxygen in photocatalytic reaction on TiO_2 .

Plausible conclusions on the mode of action of TiO_2 in photocatalytic CO_2 reduction

In contrast to the IrO_x -modified samples, the reference P25 samples exhibited a significant activity in the CH_4 formation. At the same time there was no observable activity in the H_2O splitting reaction. In general, the photocatalytic H_2O oxidation is thermodynamically possible on bare TiO_2 . Kinetic barriers in the overall reaction cycle might result in a very small apparent rate when no co-catalyst is used. Although no indication for water splitting is observed for bare TiO_2 our previous work has shown that the presence of water is required for CH_4 formation from photocatalytic CO_2 reduction. Therefore, water is still expected to deliver hydrogen for CH_4 formation. Considering that the proposed elementary steps of H_2O oxidation (5)–(8) all liberate H^+ , a hydrogen source is generated even if the final O_2 evolution step is kinetically hindered. From the results with the $\text{IrO}_x/\text{P25}$ samples it can be concluded that such a source of hydrogen should be rapidly reduced to H_2 on TiO_2 . However, on bare TiO_2 we did not observe H_2 formation, so it is questionable if any of the generally assumed steps of H_2O oxidation occurs under the applied reaction conditions. If this is not the case, a different source of protons than photocatalytic H_2O oxidation needs to participate in C–H bond formation. Moreover, the results of the present study revealed that CH_4 formation only proceeds when no H_2O is oxidized and the by-product O_2 is absent in the gas-phase. This correlation is in conflict with the proposed reaction eqn (2).

Based on our results, product formation in photocatalytic CO_2 reduction coupled to oxygen consumption by TiO_2 is suggested as likely explanation. One feasible way for such consumption is the replenishment of oxygen vacancies (O_V). From experimental studies^{53–55} it is known that O_2 dissociates and can undergo reactions with O_V on the surface of TiO_2 under room temperature conditions. Since all experiments of this study were performed under such conditions and the amount of absent O_2 is very small, it is proposed that the replenishment of O_V may explain the fate of this by-product. The obtained results of the $\text{IrO}_x/\text{P25}$ samples showed that O_2 formation started delayed to the H_2 formation. The replenishment of O_V may be the reason why fractions of O_2 were temporarily not detectable in the gas phase. Once all defects are healed the release of the entire amount of O_2 from the surface of the photocatalyst initiates, so the formation rates converged to the stoichiometric ratio of H_2O splitting. Another explanation for the initially missing gas-phase oxygen not further discussed here could be a formation of peroxide species adsorbed on the catalyst surface. The adsorption^{56,57} and reactions⁵⁷ of peroxide species, possibly also formed in a gas-phase H_2O splitting reaction on TiO_2 , has been examined in detail by comprehensive theoretical studies. Hydrogen peroxide has also been identified as origin for an oxygen deficit in liquid-phase photocatalytic water splitting over Pt/TiO_2 .⁵⁸

The overall CO_2 reduction is proposed to include two processes forming O_2 . On the one hand side the formation of

CH_4 by reduction of CO_2 , on the other hand side the oxidation of H_2O to generate the source of hydrogen for C–H bond formation. Assuming that oxygen vacancies are responsible for the absence of O_2 , these point defects are strongly associated with the photocatalytic activity of TiO_2 . In one of our studies³³ it was verified that the presence of O_2 in the gas-phase of the reaction gas atmosphere induces an inhibition of CH_4 formation. Since oxygen-derived species from CO_2 reduction are also suspected to affect the CH_4 formation negatively, a replenishment of O_V might avoid that gaseous O_2 and potentially reactive oxygen-derived intermediates inhibit the CH_4 formation.

Even though H_2O oxidation according to the generally accepted mechanism is not likely to occur on bare P25- TiO_2 , the CH_4 formation has been proven to require the presence of H_2O .³² For this reason an alternative pathway for liberation of the hydrogen in H_2O must be considered. In general, surface hydroxyl groups are naturally present on the surface of TiO_2 and can be formed by dissociative adsorption of H_2O in a O_V (11).



The surface OH-groups represent hydrogen-containing species which are available in high concentration. If they would be sufficiently Brønsted acidic to hydrogenate, for instance carbonaceous radicals as intermediates from CO_2 reduction, they could participate in product formation. Additionally, the dissociative H_2O adsorption illustrates a pathway which is consistent with the dependency of CH_4 formation from H_2O and the absence of O_2 formation.

Anyway, the irreversible replenishment of vacant positions by excess oxygen from CO_2 or H_2O is an example for a stoichiometric reaction of the photocatalyst. Most likely the photocatalytic activity in CO_2 reduction will be diminished as soon as all vacancies are healed. The observed termination of the CH_4 formation in the CO_2 reduction after 14.25 h (Fig. 6) underlines this hypothesis. Overall, the results indicate that the CH_4 formation is presumably not based on a complete catalytic cycle including both the photocatalytic CO_2 reduction and H_2O oxidation.

Experimental

High-purity gas-phase photoreactor set-up

The photocatalytic CO_2 reduction experiments were carried out with a reactor set-up which works under conditions of highest purity. A detailed description of the set-up was given by Mei *et al.*¹² In brief, the reactor is made from stainless steel components which are usually used for ultra-high vacuum application. All tube connections are realized by VCR and CF connections, so that sealing of the overall system works grease-free. Purging of the reactor is performed by 99.9999% He gas (He 6.0). A diluted CO_2 in He mixture (7000 ppm CO_2 in He 6.0) is used as the reactant gas. Dosage of H_2O into the gas-phase is realized by a stainless steel saturator, which is temperature controlled. The H_2O concentration in the gas flow is adjusted

by the temperature of the saturator. Mass flow controllers are used for purging and dosing of the reactants. The powdered sample is finely distributed in a quartz vessel, which is placed in the center of the reactor. Illumination is conducted by a 200 W Hg/Xe lamp from Oriel instruments. A water-based filter is utilized to remove the IR radiation from the lamp spectrum. Product analysis is executed by a Shimadzu Tracera GC 2010 Plus. This GC is equipped with a barrier discharge ionization detector (BID), which allows quantifying CO₂, CO, CH₄, C₂H₆, H₂O, O₂ and H₂ in the 0.1 ppm range. On the basis of this high sensitivity, the BID is a suitable analytical device for an application in continuous-flow photocatalytic CO₂ reduction.

Sample preparation

Sample modification of P25 with IrO_x and CoO_x was performed *via* photodeposition in a semi-batch reactor made from quartz glass. On-top illumination was realized by a 1000 W Hg/Xe lamp. 400 mg P25 was dispersed in 200 mL H₂O and ultrasonicated for one minute. Then the dispersion was given into the reactor and 20 mL of methanol were added. The precursors iridium acetate or cobalt acetate were added to the dispersion amounting to a nominal loading of 0.05 wt% Ir and Co, respectively. The reactor was sealed and deaerated with pure He gas for 1.5 h. After purging the reactor, the He flow rate was set to 20 mL min⁻¹ and the illumination was initiated. The overall deposition time was 3 h. Subsequently the dispersion was filtered and dried overnight. The obtained powder was then divided into two equal fractions. One fraction was calcined in synthetic air for 3 h at 200 °C, and the other at 400 °C, respectively, with a heating rate of 5 K min⁻¹. Reference samples without Ir and Co have been prepared by the same procedure. Calcination of the samples is the first step to remove adsorbed carbon-containing species from the surface to prevent their potential contribution to the product formation leading to an overestimated activity.

Sample pretreatment and CO₂ reduction

70 mg of each sample has been tested in a CO₂ reduction experiment. As the initial calcination steps are not sufficient to remove all of the carbon-containing species from the sample, further purification has been carried out before the activity test. This pretreatment step was performed in the photoreactor set-up. A He gas flow only including H₂O was given through the reactor under illumination. The flow rate of H₂O is adjusted to ~1000 nmol min⁻¹. This pretreatment under photocatalytic reaction conditions is further termed as flow cleaning. Although such an experiment is mainly performed to purify the sample from carbonaceous impurities, it simultaneously provides conditions for photocatalytic H₂O splitting. Thus the activity in the H₂O splitting reaction is determined before CO₂ reduction is studied. GC measurements are conducted all 45 minutes to monitor the cleaning progress and the formation of H₂ and O₂. After the concentration of products from the flow cleaning procedure (CH₄ and CO₂) are sufficiently low the CO₂ reduction experiment is initiated. Therefore, the gas flow is changed from pure He to 1700 nmol min⁻¹ CO₂ in He. The H₂O flow rate in the

CO₂ reduction experiments is either held at ~1000 nmol min⁻¹ or changed to ~25 nmol min⁻¹. From our previous study³² we know that high H₂O flow rates can inhibit product formation. A flow of ~25 nmol min⁻¹ H₂O is sufficient to observe significant product formation.

Conclusions

In this study the effect of improved H₂O oxidation properties on the gas-phase photocatalytic CO₂ reduction was studied by modifying P25 with co-catalysts for H₂O oxidation. Simultaneously, potential reasons for the absence of gaseous O₂ as the by-product of photocatalytic CO₂ reduction on pure TiO₂ were investigated. The IrO_x/P25 samples exhibited a significant activity in the overall photocatalytic H₂O splitting, which was realized here in a pure gas-solid process under high-purity reaction conditions. It was possible to detect both products H₂ and O₂ in nearly stoichiometric amounts without the use of sacrificial agents. Photocatalytic CO₂ reduction experiments with IrO_x/P25 samples revealed that CH₄ formation is only possible when no activity in H₂ and O₂ formation is observed. Competition for charge carriers by H₂ formation and the backward reaction of CO₂ reduction due to the presence of highly reactive oxygen species formed on IrO_x appear to be responsible for the absence of CH₄ formation. If photogenerated electrons are favorably consumed by H₂ formation, but this product is not formed on bare TiO₂, this might indicate that H₂O oxidation is not the source of hydrogen for C-H bond formation in CO₂ reduction. Furthermore, the results of the H₂O splitting experiments on IrO_x/P25 revealed that O₂ and O-derived species are initially likely consumed by TiO₂ under photocatalytic reaction conditions. A quantification of the missing amounts of O₂ in the gas phase showed that a consumption of O₂ by TiO₂ could be responsible for the absence of this by-product in the CO₂ reduction reaction. Under this circumstance TiO₂ undergoes a stoichiometric reaction and the CH₄ formation is not a true catalytic cycle. Instead, it runs only as long as TiO₂ can consume oxygen. In addition the inhibiting effect of O₂ on the product formation of CO₂ reduction reveals that the consumption of this by-product is essential for the activity of TiO₂ in this reaction. Only then the inhibiting effect of O₂ and O-derived species in the photocatalytic CO₂ reduction is prevented.

Conflicts of interest

There are no conflicts to declare.

Acknowledgements

Open Access funding provided by the Max Planck Society.

Notes and references

- 1 E. V. Kondratenko, *et al.*, *Energy Environ. Sci.*, 2013, **6**, 3112.
- 2 N. Armaroli and V. Balzani, *Energy for a sustainable world: From the oil age to a sun-powered future*, Wiley-VCH, Weinheim, 2011.



- 3 S. C. Roy, *et al.*, *ACS Nano*, 2010, **4**, 1259–1278.
- 4 R. Lal, *Energy Environ. Sci.*, 2008, **1**, 86–100.
- 5 S. Sato, T. Arai and T. Morikawa, *Inorg. Chem.*, 2015, **54**, 5105–5113.
- 6 B. Ohtani, *J. Photochem. Photobiol. C*, 2010, **11**, 157–178.
- 7 S. N. Habisreutinger, L. Schmidt-Mende and J. K. Stolarczyk, *Angew. Chem., Int. Ed.*, 2013, **52**, 7372–7408.
- 8 J. Li and N. Wu, *Catal. Sci. Technol.*, 2015, **5**, 1360–1384.
- 9 A. Di Paola, *et al.*, *J. Phys. Chem. C*, 2009, **113**, 15166–15174.
- 10 M. Anpo and J. M. Thomas, *Chem. Commun.*, 2006, 3273–3278.
- 11 J. Nowotny, *Oxide Semiconductors for Solar Energy Conversion: Titanium Dioxide*, CRC Press, 2016.
- 12 B. Mei, A. Pougin and J. Strunk, *J. Catal.*, 2013, **306**, 184–189.
- 13 M. Anpo, *et al.*, *J. Electroanal. Chem.*, 1995, **396**, 21–26.
- 14 A. Pougin, M. Dilla and J. Strunk, *Phys. Chem. Chem. Phys.*, 2016, 10809.
- 15 D. Lee and Y. Kanai, *J. Am. Chem. Soc.*, 2012, **134**, 20266–20269.
- 16 I. A. Shkrob, *et al.*, *J. Phys. Chem. C*, 2012, **116**, 9461–9471.
- 17 C. Amatore and J. M. Saveant, *J. Am. Chem. Soc.*, 1981, **103**, 5021–5023.
- 18 I. A. Shkrob, *et al.*, *J. Phys. Chem. C*, 2012, **116**, 9450–9460.
- 19 M. Anpo, *et al.*, *J. Phys. Chem. B*, 1997, **101**, 2632–2636.
- 20 N. G. Moustakas and J. Strunk, *Chem. – Eur. J.*, 2018, **24**, 12739–12746.
- 21 J. Schneider, *et al.*, *Chem. Rev.*, 2014, **114**, 9919–9986.
- 22 E. Korovin, D. Selishchev and D. Kozlov, *Top. Catal.*, 2016, **59**, 1292–1296.
- 23 K. Teramura, *et al.*, *Angew. Chem., Int. Ed.*, 2012, **51**, 8008–8011.
- 24 K. Iizuka, *et al.*, *J. Am. Chem. Soc.*, 2011, **133**, 20863–20868.
- 25 J.-C. Wang, *et al.*, *ACS Appl. Mater. Interfaces*, 2015, **7**, 8631–8639.
- 26 L. Liu, *et al.*, *ACS Catal.*, 2012, **2**, 1817–1828.
- 27 F. Saladin and I. Alxneit, *J. Chem. Soc., Faraday Trans.*, 1997, **93**, 4159–4163.
- 28 J. Tang, J. R. Durrant and D. R. Klug, *J. Am. Chem. Soc.*, 2008, **130**, 13885–13891.
- 29 H. Belhadj, *et al.*, *Phys. Chem. Chem. Phys.*, 2015, **17**, 22940–22946.
- 30 Z. Dohnalek, *et al.*, *J. Phys. Chem. B*, 2006, **110**, 6229–6235.
- 31 J. Rossmeisl, *et al.*, *J. Electroanal. Chem.*, 2007, **607**, 83–89.
- 32 M. Dilla, *et al.*, *ChemCatChem*, 2017, **9**, 4345–4352.
- 33 M. Dilla, R. Schlögl and J. Strunk, *ChemCatChem*, 2017, **9**, 696–704.
- 34 D. A. Panayotov and J. T. Yates, *Chem. Phys. Lett.*, 2005, **410**, 11–17.
- 35 R. L. Kurtz, *et al.*, *Surf. Sci.*, 1989, **218**, 178–200.
- 36 Z. Cai, *et al.*, *Adv. Energy Mater.*, 2018, **8**, 1701694.
- 37 H. Tueysuez, *et al.*, *Nano Res.*, 2013, **6**, 47–54.
- 38 C. C. L. McCrory, *et al.*, *J. Am. Chem. Soc.*, 2013, **135**, 16977–16987.
- 39 F. A. Frame, *et al.*, *J. Am. Chem. Soc.*, 2011, **133**, 7264–7267.
- 40 V. Pfeifer, *et al.*, *Chem. Sci.*, 2016, **7**, 6791–6795.
- 41 V. Pfeifer, *et al.*, *Chem. Sci.*, 2017, **8**, 2143–2149.
- 42 W.-H. Ryu, *et al.*, *J. Mater. Chem. A*, 2014, **2**, 5610–5615.
- 43 B. H. Meekins and P. V. Kamat, *J. Phys. Chem. Lett.*, 2011, **2**, 2304–2310.
- 44 Y. K. Kho, *et al.*, *J. Phys. Chem. C*, 2010, **114**, 2821–2829.
- 45 D. Y. C. Leung, *et al.*, *ChemSusChem*, 2010, **3**, 681–694.
- 46 Y.-F. Li, *et al.*, *J. Am. Chem. Soc.*, 2010, **132**, 13008–13015.
- 47 Y.-F. Li and A. Selloni, *ACS Catal.*, 2016, **6**, 4769–4774.
- 48 A. Valdes, *et al.*, *J. Phys. Chem. C*, 2008, **112**, 9872–9879.
- 49 R. van de Krol and M. Grätzel, *Photoelectrochemical Hydrogen Production*, Springer US, 2011.
- 50 J. Petlicki and T. G. M. van de Ven, *J. Chem. Soc., Faraday Trans.*, 1998, **94**, 2763–2767.
- 51 W. H. Koppenohl and J. D. Rush, *J. Phys. Chem.*, 1987, **91**, 4429–4430.
- 52 N. M. Dimitrijevic, *et al.*, *J. Am. Chem. Soc.*, 2011, **133**, 3964–3971.
- 53 M. A. Henderson, *et al.*, *J. Phys. Chem. B*, 2003, **107**, 534–545.
- 54 Y. Du, Z. Dohnalek and I. Lyubinetsky, *J. Phys. Chem. C*, 2008, **112**, 2649–2653.
- 55 S. Tan, *et al.*, *J. Am. Chem. Soc.*, 2011, **133**, 2002–2009.
- 56 H. Alghamdi, *et al.*, *Surf. Sci.*, 2018, **669**, 103–113.
- 57 W.-F. Huang, *et al.*, *J. Comput. Chem.*, 2011, **32**, 1065–1081.
- 58 V. Dascalaki, *et al.*, *Chem. Eng. J.*, 2011, **170**, 433–439.

